Electronic Supplementary Material (ESI) for ChemComm.


# Supplementary Information

# Unexplored reactivity of $(S_n)^{2-}$ Oligomers with transition metals in low-temperature solid-state reactions

*Shunsuke Sasaki, Melanie Lesault, Elodie Grange, Etienne Janod, Benoît Corraze, Sylvian Cadars, Maria Teresa Caldes, Catherine Guillot-Deudon, Stéphane Jobic* and Laurent Cario**

*Institut des Matériaux Jean Rouxel (IMN), Université de Nantes, CNRS, 2 rue de la Houssinière, BP 32229, 44322 Nantes Cedex 3, France.*

*E-mail. Stephane.Jobic@cnrs-imn.fr, Laurent.Cario@cnrs-imn.fr

**Table of Contents**

# Experimental procedures

## 1. Synthetic procedures

*Barium disulfide $BaS_2$*

To remove the trace amount of impurities, the grey powder of BaS (Aldrich, 99.9%) was treated under 5% $H_2$/Ar flow at 850 °C for 48 h beforehand. The obtained white powder of BaS was combined with S flakes (Aldrich, 99.99+%) in BaS : S = 1 : 1.005 molar ratio and ground in an agate mortar under argon atmosphere. Then the mixture was pelletized and sealed in an evacuated (~$10^{-3}$ torr) silica tube. The sealed mixture was heated to 600 °C at a rate of 100 °C $h^{-1}$ and annealed for 48 h. Finally the sealed mixture was gradually cooled in a furnace to afford the yellow pellet. XRD pattern of the obtained mixture well with the previous report[1] without any impurity phase.

*Barium trisulfide $BaS_3$*

Beforehand BaS (Aldrich, 99.9%) was treated in the same way with the $BaS_2$ synthesis. The obtained white powder of BaS was combined with S flakes (Aldrich, 99.99+%) in BaS : S = 1 : 2.05 molar ratio and ground in an agate mortar under argon atmosphere. Then the mixture was pelletized and sealed in an evacuated (~$10^{-3}$ torr) silica tube. The sealed mixture was heated to 500 °C at a rate of 50 °C $h^{-1}$ and annealed for 12 h. Finally the sealed mixture was gradually cooled in a furnace to afford the vivid yellow pellet while surplus sulfur was deposited on the opposite side of the silica tube. XRD pattern of the obtained mixture well with the previous report[2] without any impurity phase.

*Insertion of Cu into $BaS_2$ and $BaS_3$*

Syntheses of the precursors $BaS_2$ and $BaS_3$ are described above. $BaS_2$ and Cu (Alfa Aesar, 100-325 mesh, 99.9%) were weighted in 1 : 2 molar ratio and their mixture was ground in an agate mortar under argon atmosphere. Then the mixture was pelletized and sealed in an evacuated (~$10^{-3}$ torr) silica tube. The sealed mixture was heated to 240 °C at a rate of 300 °C $h^{-1}$ and annealed for 4 h, followed by gradual cooling. The obtained brown pellet was crushed, pelletized and then heated again in the same way with the first treatment, to afford the brown pellet of $BaCu_2S_2$. $BaCu_4S_3$ was prepared in the same way from the mixture of $BaS_3$ and Cu in 1 : 4 molar ratio.

*Insertion of Ni into $BaS_2$*

Syntheses of the precursor $BaS_2$ is described above. $BaS_2$ and Ni (Aldrich, nanopowder with <100 nm in the average size, ≥99%) were weighted in 1 : 1 molar ratio and their mixture was ground in an agate mortar under argon atmosphere. Then the mixture was pelletized and sealed in an evacuated (~$10^{-3}$ torr) silica tube. The sealed mixture was heated to 340 °C at a rate of 300 °C $h^{-1}$ and annealed for 12 h. Finally the sealed mixture was gradually cooled in a furnace to afford the mixture of $BaNiS_2$, BaS and NiS as the black pellet (See Fig. 3b, S10 and Table S3). Neither different initial temperature of the thermal treatment (e.g. 240 and 300 °C instead of r.t.), the use of larger Ni particles (Alfa Aesar, 125 mesh, 99.996%) nor the shorter duration of annealing (e.g. 2 h) affected the consequence of the reaction. On the other hand, the lower reaction temperature (e.g. 240, 265 and 280 °C) diminished XRD peaks of $BaNiS_2$.

*Reaction between Ni and $BaS_3$*

Syntheses of the precursor $BaS_3$ is described above. $BaS_3$ and Ni (Alfa Aesar, ~120 mesh, 99.996%) were weighted in 1 : 2 molar ratio and their mixture was ground in an agate mortar under argon atmosphere. Then the mixture was pelletized and sealed in an evacuated (~$10^{-3}$ torr) silica tube. The sealed tube was inserted into the furnace preheated at 300 °C. Then the mixture was further heated to 340 °C at a rate of 300 °C $h^{-1}$ and annealed for 1 h. Finally the sealed mixture was quenched to afford the lustering grey pellet of $BaNiS_2$ and NiS as well as trace amounts of BaS (See Fig. 3b, S11).

*Insertion of Fe into $BaS_3$*

Syntheses of the precursor $BaS_3$ is described above. $BaS_3$ and Fe (Alfa Aesar, ~22 mesh, 99.998%) were weighted in 1 : 2 molar ratio and their mixture was ground in an agate mortar under argon atmosphere. Then the mixture was pelletized and sealed in an evacuated (~$10^{-3}$ torr) silica tube. The sealed tube was inserted into the furnace preheated at 300 °C. Then the mixture was further heated to 340 °C at a rate of 300 °C $h^{-1}$ and annealed for 1 h. Finally the sealed mixture was quenched to afford the black pellet of $BaFe_2S_3$ as well as trace amounts of FeS and $Ba_6Fe_8S_{15}$ (See Fig. 3d, S12 and Table S4). Higher initial temperature (e.g. 340 °C) or the use of Fe nanoparticles (Aldrich, 35-45 nm in particle size, 99.5%) led the preferential formation of $Ba_6Fe_8S_{15}$. On the other hand, lower initial temperature (below 285 °C) resulted in the severe competition with the decomposition into BaS and FeS.

## 2. Characterization

Powder X-ray diffraction (XRD) patterns were recorded at room temperature on a Bruker D8 Advance Diffractometer (Bragg-Brentano geometry, $\theta$-$2\theta$), which employs Cu $K_{\alpha 1}$ radiation ($\lambda$ = 1.540598 Å) produced through Ge (111) monochromator and a LynxEye detector. Rietveld refinements of these XRD patterns were performed with Jana2006 package[3] on the basis of the previously reported structure models[1-2,4-11] using the fundamental parameter approach.[12] Raman spectra were recorded in a backscattering geometry with a 514 nm argon laser using either Renishaw inVia Raman spectrometer. For all measurements, the laser power was adjusted to 0.15 mW on the sample and at least two different points on powder samples are analyzed to ensure homogeneity of samples.

# Results and Discussions

### 1. Electronic structure of $BaS_3$

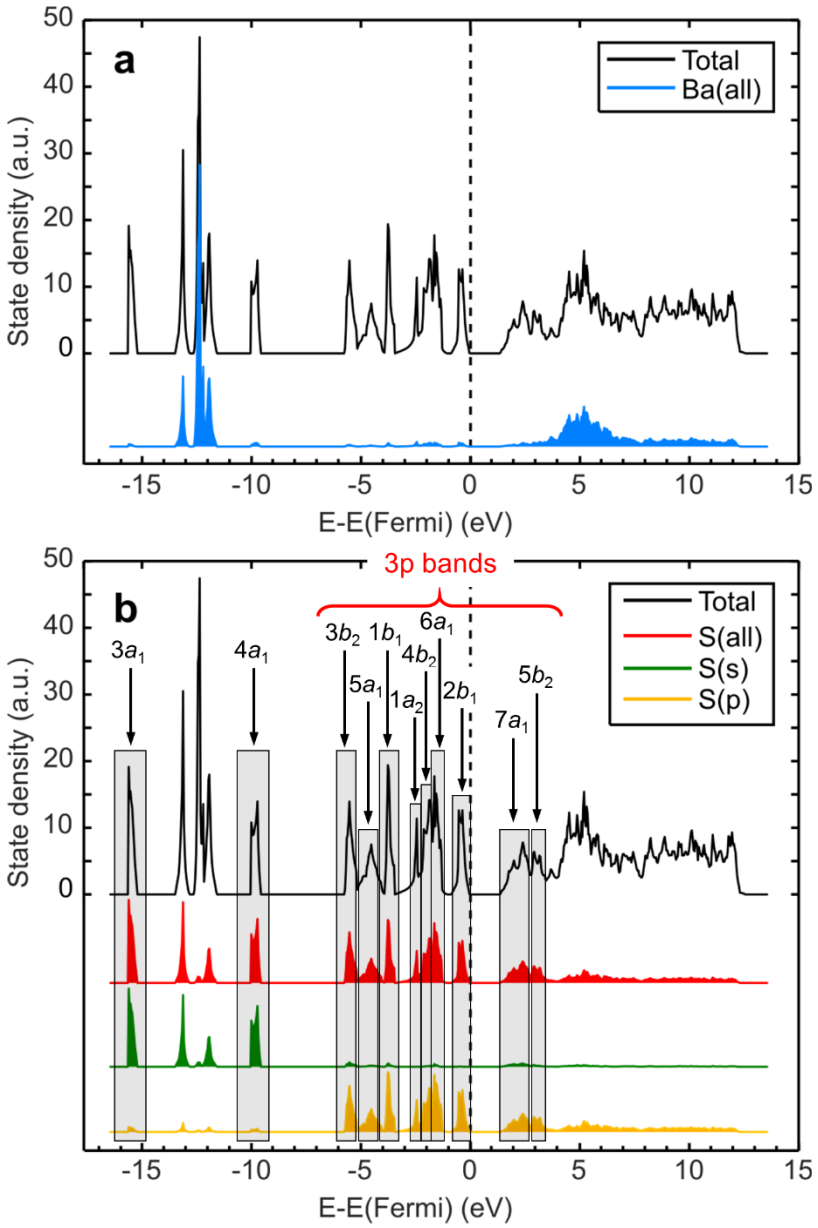


**Figure S1.** Total and atomic projected density of states around the Fermi level $E_F$ calculated for $BaS_3$. Energy bands composed exclusively by s and p orbitals of sulfur atoms are shaded in grey. Each of these shaded bands exhibited an isosurface similar with each molecular orbital of isolated triatomic molecules that were made of p-block element (e.g. $CO_2$, $O_3$, etc…).[13-14] Accordingly each 3p band was labelled following the assignment for these molecular orbitals. The order of these 3p bands accords well with the electronic configuration of the neutral and the isolated $S_3$ molecule.[15]

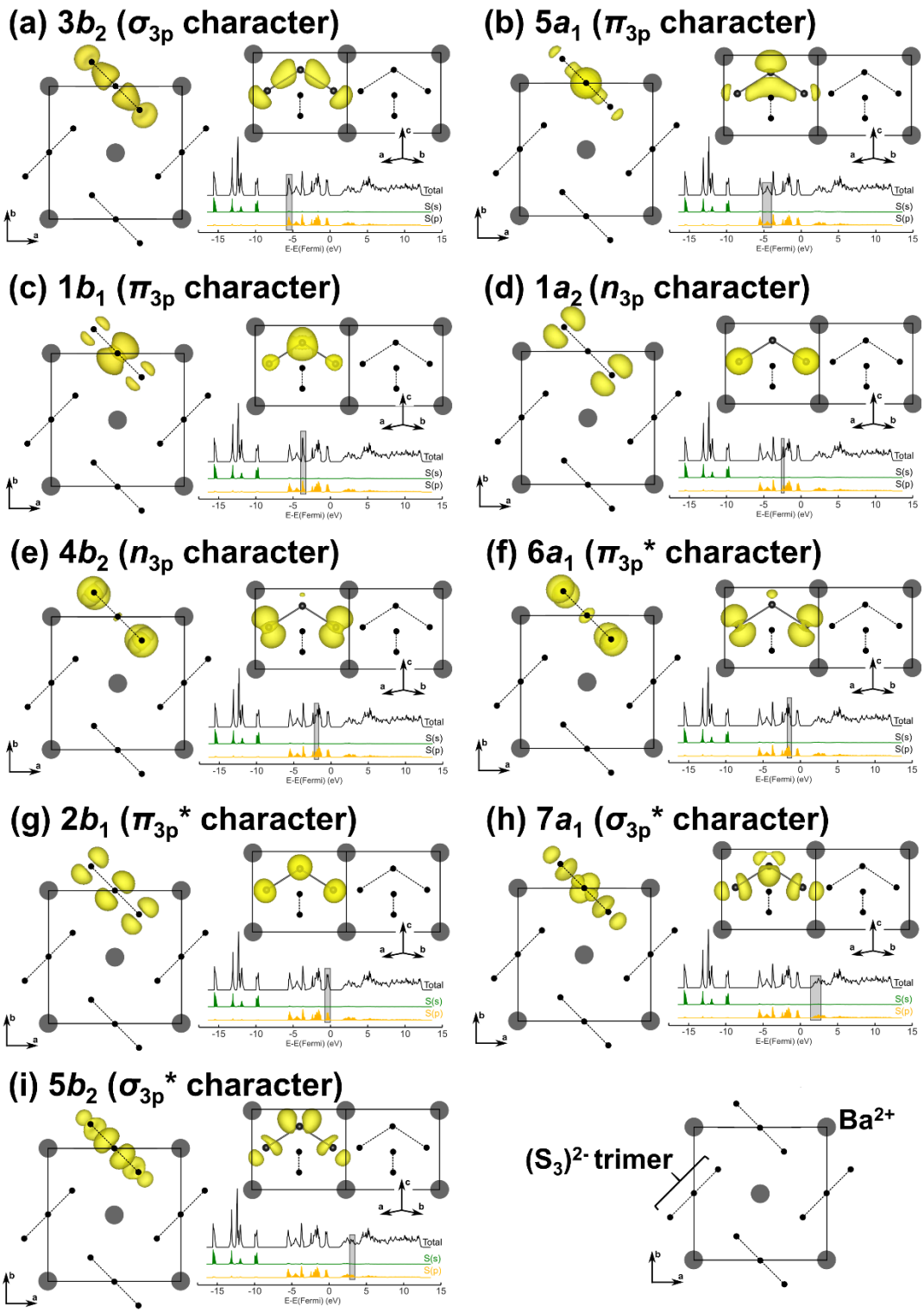


**Figure S2.** Isosurfaces of partial charge density around a $(S_3)^{2-}$ trimer embedded in $BaS_3$. Each isosurface was extracted from the energy range shaded by grey in the density of state diagram (See Figure S1 for the detail of energy range). Each isosurface was assigned by the similarity in its shape with the molecular orbitals of isolated $O_3$ and $S_3$ molecules.[14,15]

## 2. Insertion of Cu into $BaS_2$ and $BaS_3$

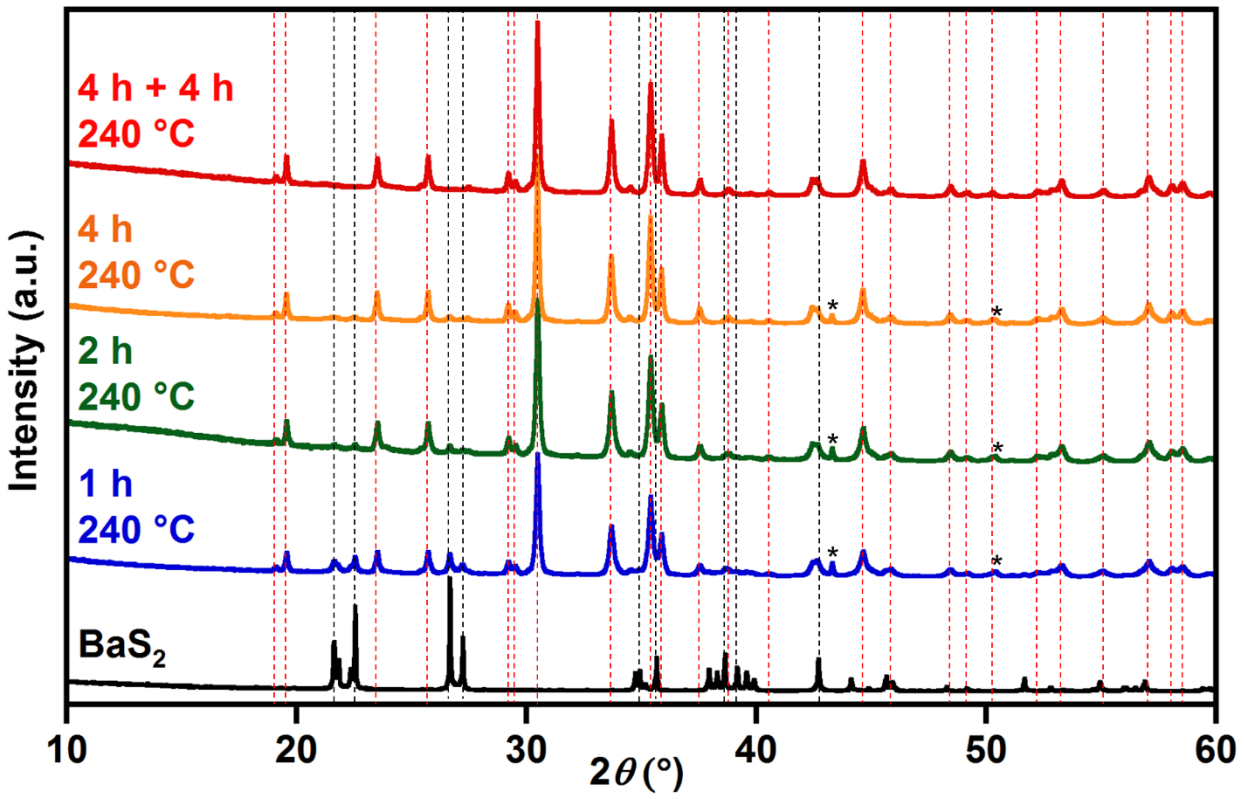


**Figure S3.** XRD patterns of $BaS_2$ and the $BaS_2$ + 2Cu mixtures after thermal treatments for different durations. The * marks signify the XRD peak of Cu.

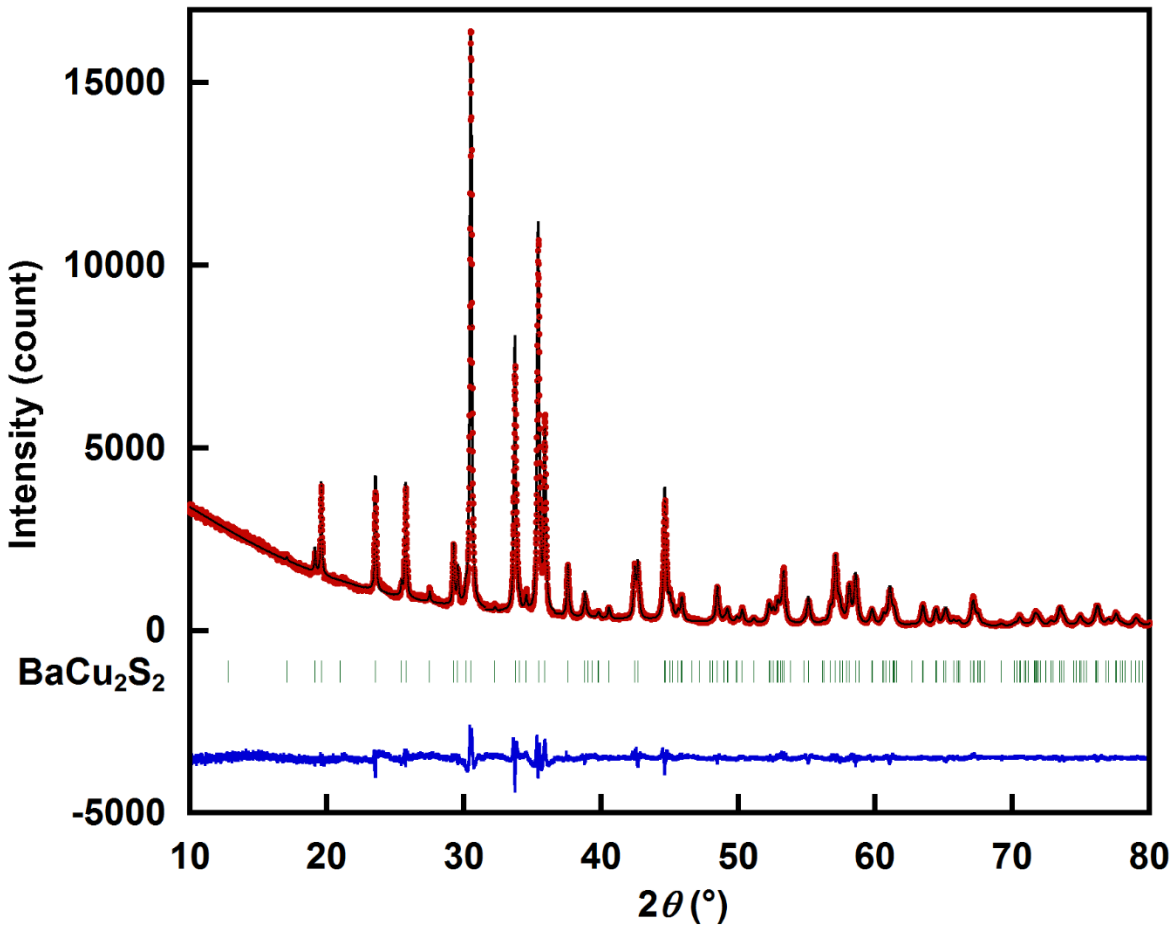


**Figure S4**. Rietveld refinement of $BaCu_2S_2$ prepared from the mixture $BaS_2$ + 2.0 Cu. The mixture underwent two thermal treatments at 240 °C for 4 h intersected by a manual milling step. Observed, calculated profiles and their difference are drawn by red, black and blue lines, respectively. The vertical green bars indicate the position of Bragg reflections.

**Table S1**. Crystallographic parameters determined from Rietveld refinement of $BaCu_2S_2$ powder prepared from the mixture $BaS_2$ + 2.0 Cu. The mixture underwent two thermal treatments at 240 °C for 4 h intersected by a manual milling step.

| | |
|---|---|
| *Crystallographic and physical data* | |
| Chemical formula | $BaCu_2S_2$ |
| Molar mass (g $mol^{-1}$) | 328.54 |
| Symmetry | Orthorhombic |
| Color | Brown |
| Space group | *Pnma* (No. 62) |
| *a* (Å) | 9.2756(1) |
| *b* (Å) | 4.0567(2) |
| *c* (Å) | 10.3857(7) |
| Volume ($Å^3$) | 390.80(1) |
| *Z* | 4 |
| Density (g $cm^{-3}$) | 5.5842 |
| *Structural refinement* | |
| Reliability factors | $R_p$ = 4.47%; *R*(obs) = 2.12%; *R*(all) = 2.13% |
| Weighted reliability factors | $_wR_p$ = 6.18%; $_wR$(obs) = $_wR$(all) = 3.37% |
| Goodness of fit | 1.82 |

*Atomic positions and isotropic thermal parameters*[a]

| Atom | *x* | *y* | *z* | $U_{iso}$ ($Å^2$) |
|---|---|---|---|---|
| Ba | 0.2606(9) | 0.75 | 0.3239(8) | 0.0078(5) |
| Cu1 | 0.0556(7) | 0.25 | 0.1107(7) | 0.0100(8) |
| Cu2 | 0.4145(0) | 0.75 | 0.0425(3) | 0.0147(1) |
| S1 | 0.4806(2) | 0.25 | 0.1692(4) | 0.0031(7) |
| S2 | 0.1571(2) | 0.75 | 0.0421(1) | 0.0122(9) |

[a] Site-occupancy factors of all atoms are fixed to full occupancy.

[b] The refinements of $BaS_2$, Cu and $BaCu_2S_2$ were performed on the basis of the structural models reported in the reference [1], [4] and [5], respectively.

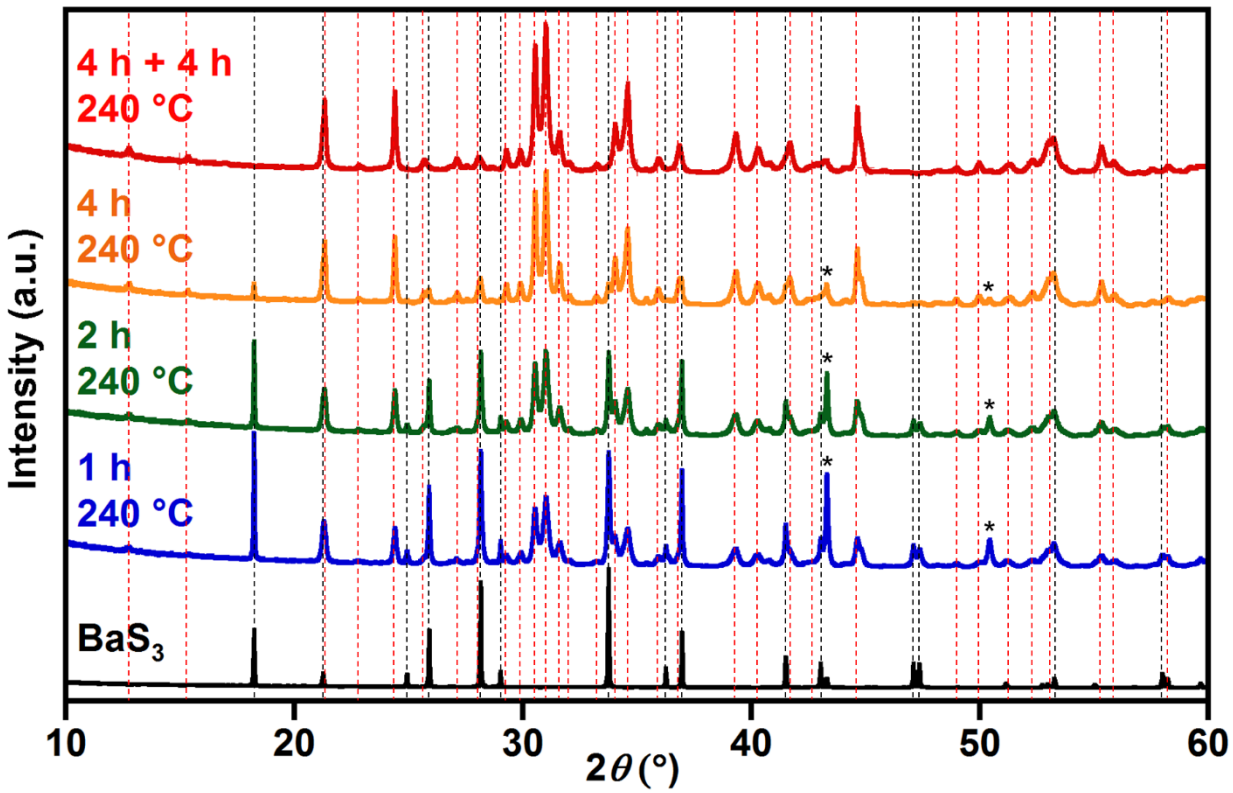


**Figure S5.** XRD patterns of $BaS_3$ and the $BaS_3$ + 4Cu mixtures after thermal treatments for different durations. The * marks signify the XRD peak of Cu.

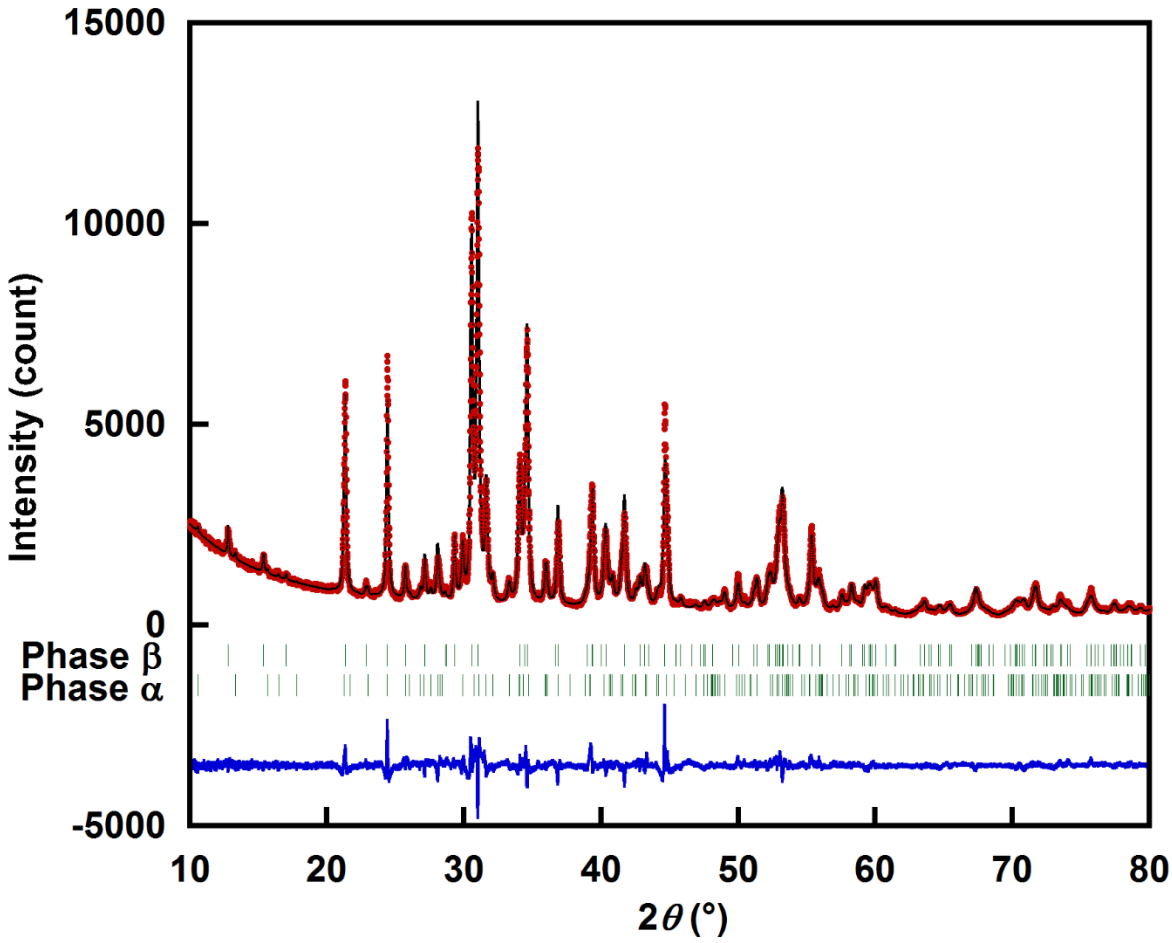


**Figure S6**. Rietveld refinement of $BaCu_4S_3$ prepared from the mixture $BaS_3$ + 4.0 Cu. The mixture underwent two thermal treatments at 240 °C for 4 h intersected by a manual milling step. Observed, calculated profiles and their difference are drawn by red, black and blue lines, respectively. The vertical green bars indicate the position of Bragg reflections.

**Table S2**. Crystallographic parameters determined from Rietveld refinement of $BaCu_4S_3$ powder prepared from the mixture $BaS_3$ + 4.0 Cu. The mixture underwent two thermal treatments at 240 °C for 4 h intersected by a manual milling step.

| | |
|---|---|
| *Basic data* | |
| Chemical formula | $BaCu_4S_3$ |
| Molar mass (g mol$^{-1}$) | 487.69 |
| Color | Dark-brown |
| | |
| *Structural refinement* – ***Profile*** | |
| Reliability factors | $R_p$ = 5.15% |
| Weighted reliability factors | $_wR_p$ = 6.95% |
| Goodness of fit | 2.13 |
| | |
| *Crystallographic data* – ***Phase alpha*** | |
| Symmetry | Orthorhombic |
| Space group | *Pnma* (No. 62) |
| *a* (Å) | 10.7633(9) |
| *b* (Å) | 4.0457(5) |
| *c* (Å) | 13.2960(1) |
| Volume (Å$^3$) | 578.98(7) |
| *Z* | 4 |
| Density (g cm$^{-3}$) | 5.5950 |
| Mass fraction | 0.359 |
| | |
| *Structural refinement* – ***Phase alpha*** | |
| Reliability factors | *R*(obs) = 2.98%; *R*(all) = 3.01% |
| Weighted reliability factors | $_wR$(obs) = $_wR$(all) = 3.94% |

*Atomic positions and isotropic thermal parameters* – ***Phase alpha*** [a]

| Atom | *x* | *y* | *z* | $U_{iso}$ (Å$^2$) |
|---|---|---|---|---|
| Ba | 0.2256(4) | 0.25 | 0.0188(9) | 0.0266(1) |
| S1 | 0.0453(3) | 0.75 | 0.1141(5) | 0.0025[b] |
| S2 | 0.4261(7) | 0.75 | 0.0966(8) | 0.0025[b] |
| S3 | 0.2317(2) | 0.25 | 0.3272(3) | 0.0278(1) |
| Cu1 | 0.4506(5) | 0.25 | 0.3346(4) | 0.0727(8) |
| Cu2 | 0.3262(4) | 0.75 | 0.2512(9) | 0.0168(3) |
| Cu3 | 0.0916(4) | 0.75 | 0.2729(3) | 0.1405(4) |
| Cu4 | 0.0336(9) | 0.25 | 0.4015(6) | 0.0869(0) |

| | |
|---|---|
| *Crystallographic data* – ***Phase beta*** | |
| Symmetry | Orthorhombic |
| Space group | *Cmcm* (No. 63) |
| *a* (Å) | 4.0561(0) |
| *b* (Å) | 13.8456(8) |
| *c* (Å) | 10.4169(2) |
| Volume (Å$^3$) | 585.00(8) |
| *Z* | 4 |
| Density (g cm$^{-3}$) | 5.5374 |
| Mass fraction | 0.641 |

*Structural refinement* – ***Phase beta***

| | |
|---|---|
| Reliability factors | $R$(obs) = $R$(all) = 2.87% |
| Weighted reliability factors | $_wR$(obs) = $_wR$(all) = 4.30% |

*Atomic positions and isotropic thermal parameters* – ***Phase beta*** [a]

| Atom | *x* | *y* | *z* | $U_{iso}$ (Å$^2$) |
|---|---|---|---|---|
| Ba | 0 | 0.2440(0) | 0.25 | 0.0355(4) |
| S1 | 0.5 | 0.1490(0) | 0.4517(1) | 0.0323(7) |
| S2 | 0 | 0.0686(9) | 0.75 | 0.0387(2) |
| Cu1 | 0 | 0.1081(8) | 0.5310(9) | 0.0468(1) |
| Cu2 | 0.5 | -0.0002(1) | 0.3719(2) | 0.1071(1) |

[a] Site-occupancy factors of all atoms are fixed to full occupancy.

[b] The refinements of $BaS_3$, Cu and $BaCu_4S_3$ were performed on the basis of the structural models reported in the reference [2], [4] and [6], respectively.

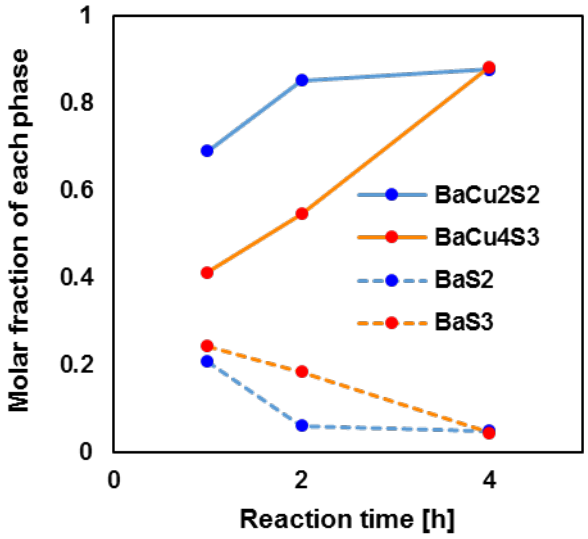


**Figure S7**. Molar fraction of each ternary phase and each $BaS_n$ precursor plotted over duration of thermal treatments. Molar fraction of these phases was estimated by Rietveld refinements.

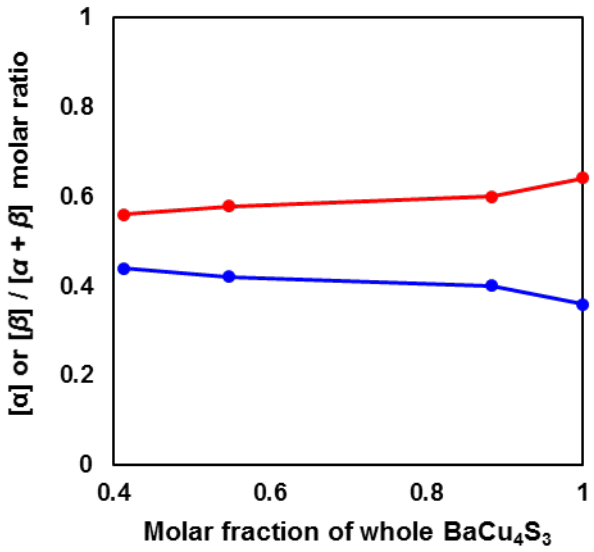


**Figure S8**. Relative ratio between *α* and *β*-$BaCu_4S_3$ phases in the mixture $BaS_3$ + 4.0 Cu after 1, 2, 4 and 4 + 4 h of thermal treatment. Molar fraction of *α* and *β*-$BaCu_4S_3$, $BaS_3$ and Cu was estimated by Rietveld refinement.

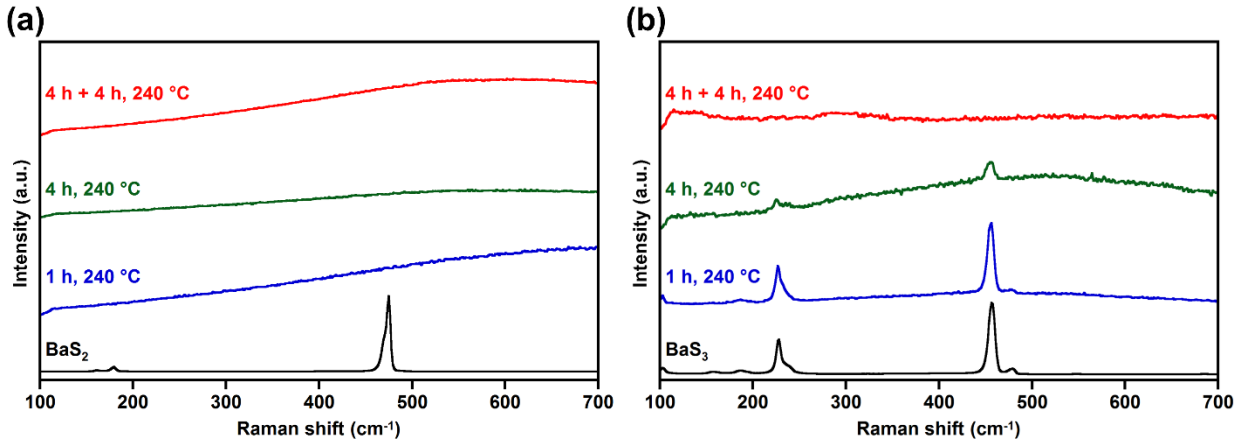


**Figure S9**. Raman spectra of the $BaS_2$ + 2Cu and $BaS_3$ + 4Cu mixtures after thermal treatment at 240 °C, respectively.

### 3. Insertion of Ni and Fe into $BaS_2$ and $BaS_3$

**Table S3**. Crystallographic parameters determined from Rietveld refinement of the mixture $BaS_2$ + 1.0 Ni after the thermal treatments at 340 °C for 12 h.

| | |
|---|---|
| *Basic data* | |
| Color | Black |
| | |
| *Structural refinement* – ***Profile*** | |
| Reliability factors | $R_p$ = 7.08% |
| Weighted reliability factors | $_wR_p$ = 9.53% |
| Goodness of fit | 1.65 |
| | |
| *Crystallographic data* – ***$BaNiS_2$*** | |
| Chemical formula | $BaNiS_2$ |
| Molar mass (g mol$^{-1}$) | 260.14 |
| Symmetry | Tetragonal |
| Space group | *P*4/*nmm* (No. 129) |
| *a* (Å) | 4.4496(9) |
| *c* (Å) | 8.9254(8) |
| Volume (Å$^3$) | 176.72(2) |
| *Z* | 2 |
| Density (g cm$^{-3}$) | 4.8889 |
| Mass fraction | 0.413 |
| | |
| *Structural refinement* – ***$BaNiS_2$*** | |
| Reliability factors | *R*(obs) = *R*(all) = 3.82% |
| Weighted reliability factors | $_wR$(obs) = $_wR$(all) = 4.05% |

*Atomic positions and isotropic thermal parameters* – ***$BaNiS_2$*** [a]

| Atom | *x* | *y* | *z* | $U_{iso}$ (Å$^2$) |
|---|---|---|---|---|
| Ba | 0.25 | 0.25 | 0.8134(9) | 0.0127(1) |
| Ni | 0.25 | 0.25 | 0.4114(3) | 0.0108(8) |
| S1 | 0.25 | 0.25 | 0.1437(6) | 0.001[b] |
| S2 | 0.75 | 0.25 | 0.5 | 0.0612(8) |

| | |
|---|---|
| *Crystallographic data* – ***BaS*** | |
| Chemical formula | BaS |
| Molar mass (g mol$^{-1}$) | 169.39 |
| Symmetry | Cubic |
| Space group | *Fm*-3*m* (No. 225) |
| *a* (Å) | 6.3891(1) |
| Volume (Å$^3$) | 260.80(8) |
| *Z* | 4 |
| Density (g cm$^{-3}$) | 4.3141 |
| Mass fraction | 0.309 |
| | |
| *Structural refinement* – ***BaS*** | |
| Reliability factors | *R*(obs) = *R*(all) = 1.20% |

| | |
|---|---|
| Weighted reliability factors | $_wR$(obs) = $_wR$(all) = 1.63% |

*Atomic positions and isotropic thermal parameters – **BaS*** [a]

| Atom | *x* | *y* | *z* | $U_{iso}$ (Å$^2$) |
|---|---|---|---|---|
| Ba | 0 | 0 | 0 | 0.0038(9) |
| S | 0.5 | 0.5 | 0.5 | 0.0105(4) |

*Crystallographic data – **NiS***

| | |
|---|---|
| Chemical formula | NiS |
| Molar mass (g mol$^{-1}$) | 90.75 |
| Symmetry | Hexagonal |
| Space group | $P6_3/mmc$ (No. 194) |
| *a* (Å) | 3.4315(1) |
| *c* (Å) | 5.3288(1) |
| Volume (Å$^3$) | 54.34(1) |
| *Z* | 2 |
| Density (g cm$^{-3}$) | 5.5462 |
| Mass fraction | 0.283 |

*Atomic positions and isotropic thermal parameters – **NiS*** [a]

| Atom | *x* | *y* | *z* | $U_{iso}$ (Å$^2$) |
|---|---|---|---|---|
| Ni | 0 | 0 | 0 | 0.0335(6) |
| S | 1/3 | 2/3 | 0.25 | 0.001[b] |

[a] Site-occupancy factors of all atoms are fixed to full occupancy.

[b] These atomic displacement factors are fixed to 0.001.

[c] The refinements of $BaNiS_2$, BaS and NiS were performed on the basis of the structural models reported in the reference [7], [8] and [9], respectively.

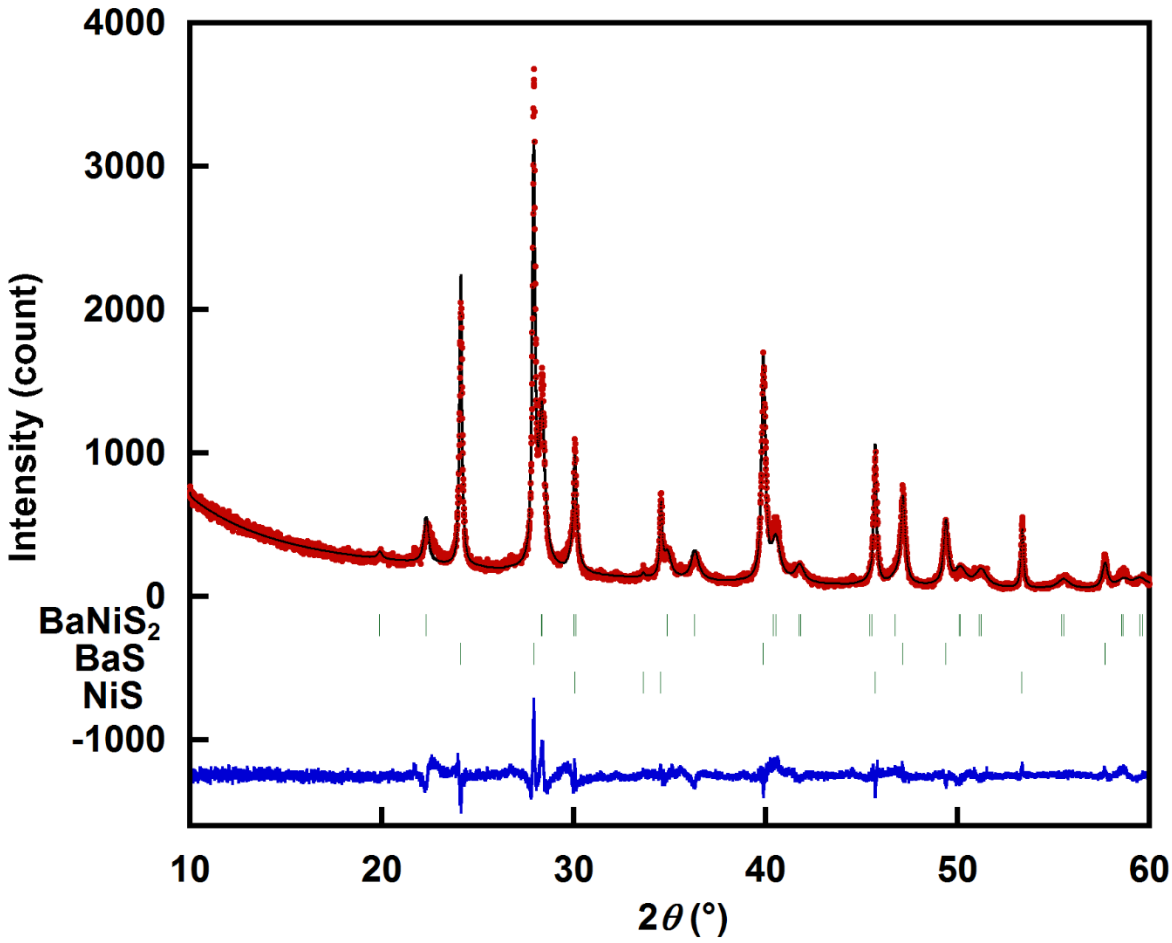


**Figure S10**. Rietveld refinement of the mixture $BaS_2$ + 1.0 Ni after the thermal treatments at 340 °C for 12 h. Observed, calculated profiles and their difference are drawn by red, black and blue lines, respectively. The vertical green bars indicate the position of Bragg reflections.

As a follow-up experiment (Fig. S11), the mixture of $BaS_3$ and Ni in 1:1 molar ratio was subject to the same thermal treatment: introduction into the preheated furnace and subsequent annealing for 1 h. This attempt with less amount of Ni ended up in the formation of $BaS_2$ and hexagonal NiS as the major products while BaS and $NiS_2$ were also observed as minor phases. Thus the reaction between Ni and $BaS_3$ firstly gave the mixture of $BaS_2$ and NiS.

As shown in the main text, further reaction of $BaS_2$ with Ni led the formation of the desired phase $BaNiS_2$. In contrast to the case of $BaS_3$:Ni = 1:1 mixture, two equivalent of nickel formed many variants of NiS phases, including not only two polymorphs of NiS (SG: $P6_3/mmc$ and $R3m$), but also metastable $Ni_xS$ ($x$ ~ 1) phase, whose composition was close to $Ni_7S_6$ but structure has not been fully characterized yet.[19] The fact implies that the reaction between $BaS_2$ produced in-situ and Ni remained affected stability of each NiS phase. The amount of each phase quantified by our Rietveld refinement was 75 wt% for $BaNiS_2$, 6 wt% for BaS, 10 wt% for hexagonal NiS, and 9 wt% for Rhombohedral NiS. $Ni_xS$ ($x$ ~ 1) phase could not be taken into account due to the lack of structural data.

Accordingly, the major reaction between Ni and $BaS_3$ can be explained by the following formula: $BaS_3 + 2Ni \rightarrow 0.9BaS_2 + 0.9\ Ni + 1.1\ NiS\ (+\ 0.1\ BaS) \rightarrow 0.9BaNiS_2 + 1.1\ NiS\ (+\ 0.1\ BaS)$.

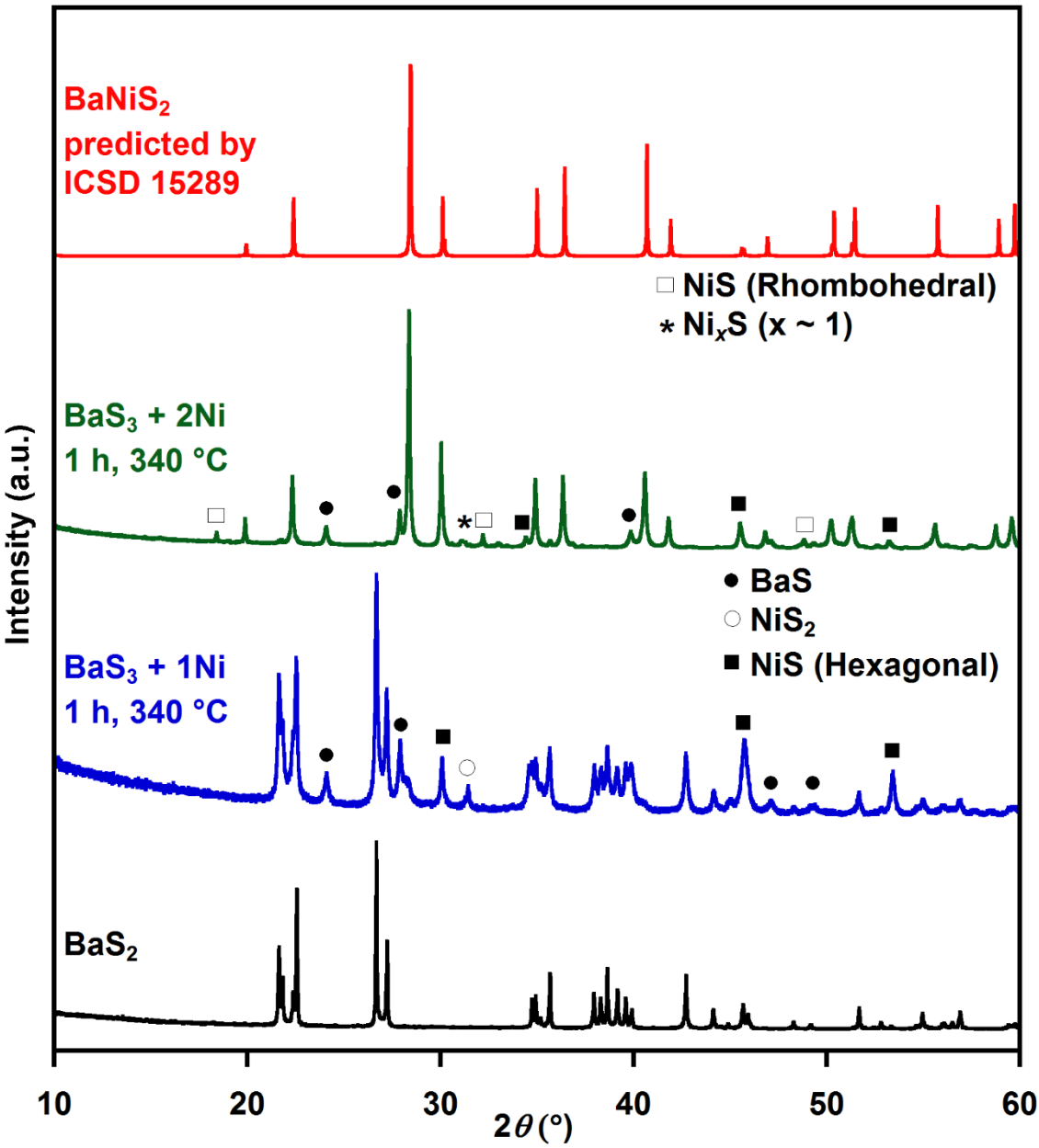


**Figure S11**. Theoretical XRD pattern of $BaNiS_2$ (red),[7] experimental XRD patterns of the $BaS_3$ + 2Ni (green) and the $BaS_3$ + Ni (blue) mixtures after the thermal treatment at 340 °C for 1 h, respectively. Experimental XRD pattern of pure $BaS_2$ was also shown. NiS (Hexagonal),[9] NiS (Rhombohedral),[17] $NiS_2$[18] are assigned based on the reported structural data. Many small peals ascribed to the metastable $Ni_xS$ (x ~ 1) phase are assigned by the cell parameters given by Seim et al.[19]

**Table S4**. Crystallographic parameters determined from Rietveld refinement of the mixture $BaS_3$ + 2.0 Fe after the thermal treatments at 340 °C for 1 h.

| | | | | |
|---|---|---|---|---|
| *Basic data* | | | | |
| Color | | Black | | |
| | | | | |
| *Structural refinement* – ***Profile*** | | | | |
| Reliability factors | | $R_p$ = 3.53% | | |
| Weighted reliability factors | | $_wR_p$ = 4.70% | | |
| Goodness of fit | | 1.82 | | |
| | | | | |
| *Crystallographic data* – ***$BaFe_2S_3$***[a] | | | | |
| Chemical formula | | $BaFe_2S_3$ | | |
| Molar mass (g mol$^{-1}$) | | 345.19 | | |
| Symmetry | | Orthorhombic | | |
| Space group | | *Cmcm* (No. 63) | | |
| *a* (Å) | | 8.7863(7) | | |
| *b* (Å) | | 11.2334(2) | | |
| *c* (Å) | | 5.2893(2) | | |
| Volume (Å$^3$) | | 522.06(2) | | |
| *Z* | | 4 | | |
| Density (g cm$^{-3}$) | | 4.3921 | | |
| Mass fraction | | 0.905 | | |
| | | | | |
| *Structural refinement* – ***$BaFe_2S_3$*** | | | | |
| Reliability factors | | *R*(obs) = 2.98%; *R*(all) = 3.00% | | |
| Weighted reliability factors | | $_wR$(obs) = 4.12%; $_wR$(all) = 4.13% | | |
| | | | | |
| *Atomic positions and isotropic thermal parameters* – ***$BaFe_2S_3$***[b] | | | | |
| Atom | *x* | *y* | *z* | $U_{iso}$ (Å$^2$) |
| Ba | 0.5 | 0.1859(8) | 0.25 | 0.0240(8) |
| Fe | 0.3451(3) | 0.5 | 0 | 0.0068(8) |
| S1 | 0.5 | 0.6162(5) | 0.25 | 0.001[c] |
| S2 | 0.2060(1) | 0.3811(9) | 0.25 | 0.0132(0) |
| | | | | |
| *Crystallographic data* – ***$Ba_6Fe_8S_{15}$*** | | | | |
| Chemical formula | | $Ba_6Fe_8S_{15}$ | | |
| Molar mass (g mol$^{-1}$) | | 1751.61 | | |
| Symmetry | | Tetragonal | | |
| Space group | | *I*4/*m* (No. 87) | | |
| *a* (Å) | | 11.4341(5) | | |
| *c* (Å) | | 10.2766(2) | | |
| Volume (Å$^3$) | | 1343.56(4) | | |
| *Z* | | 2 | | |
| Density (g cm$^{-3}$) | | 4.3300 | | |
| Mass fraction | | 0.058 | | |
| | | | | |
| *Structural refinement* – ***$Ba_6Fe_8S_{15}$*** | | | | |
| Reliability factors | | *R*(obs) = 8.32%; *R*(all) = 9.62% | | |
| Weighted reliability factors | | $_wR$(obs) = 5.40%; $_wR$(all) = 5.47% | | |

*Atomic positions and isotropic thermal parameters – **$Ba_6Fe_8S_{15}$*** [d]

*Crystallographic data – **FeS***

| | |
|---|---|
| Chemical formula | FeS |
| Molar mass (g $mol^{-1}$) | 87.90 |
| Symmetry | Hexagonal |
| Space group | P-62*c* (No. 190) |
| *a* (Å) | 5.9680 [e] |
| *c* (Å) | 11.7400 [e] |
| Volume ($Å^3$) | 362.12 [e] |
| *Z* | 12 |
| Density (g $cm^{-3}$) | 4.8372 [e] |
| Mass fraction | 0.038 |

*Atomic positions and isotropic thermal parameters – **FeS*** [d]

[a] Preferred orientation was taken into account.

[b] Site-occupancy factors of all atoms are fixed to full occupancy.

[c] These atomic displacement factors are fixed to 0.001.

[d] All the atomic parameters for $Ba_6Fe_8S_{15}$ and FeS are fixed to the reported value.[10-11]

[e] Cell parameters of FeS was fixed to the reported value.[11]

[f] The refinements of $BaFe_2S_3$, $Ba_6Fe_8S_{15}$, FeS were performed on the basis of the structural models reported in the reference [10] and [11], respectively.

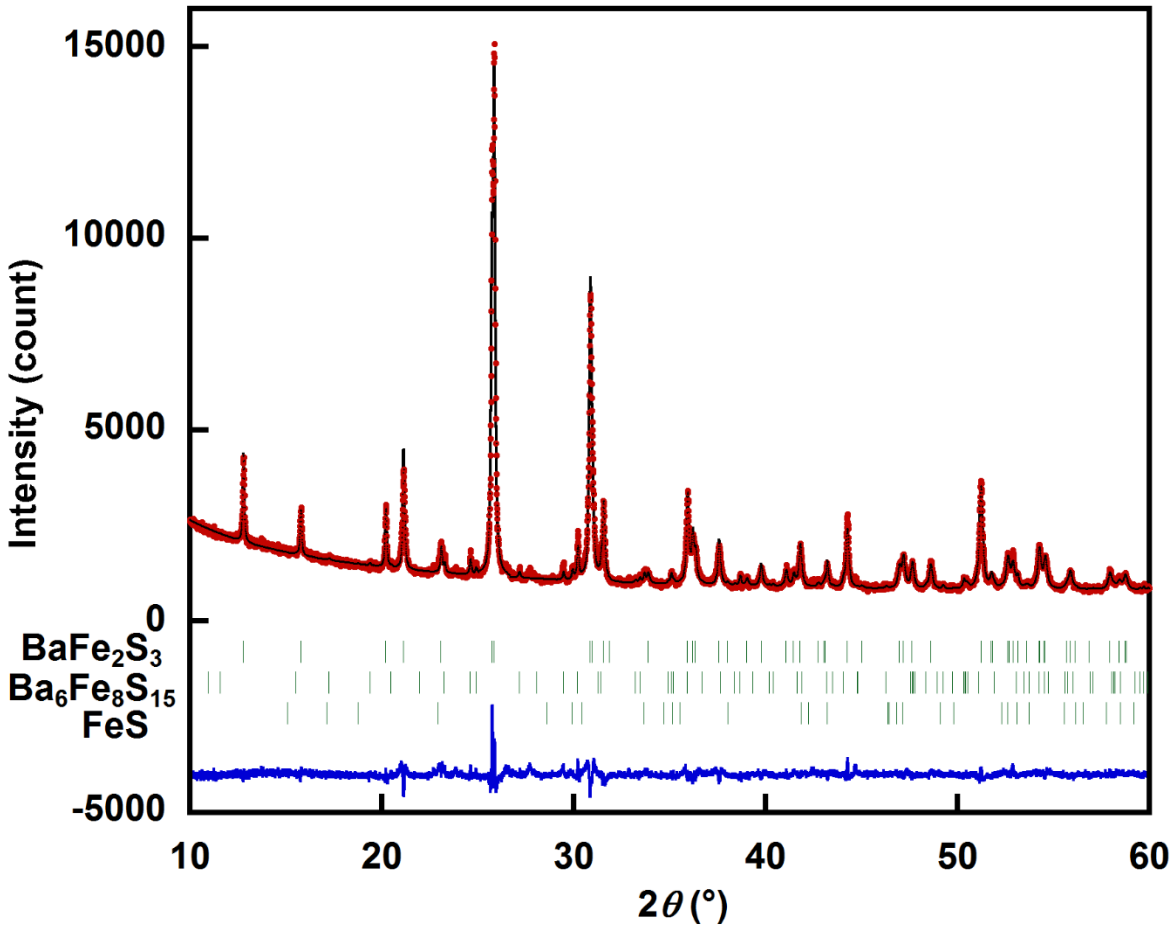


**Figure S12**. Rietveld refinement of the mixture $BaS_3$ + 2.0 Fe after the thermal treatments at 340 °C for 1 h. Observed, calculated profiles and their difference are drawn by red, black and blue lines, respectively. The vertical green bars indicate the position of Bragg reflections.

## 4. Plausible pathway of the phase transformations

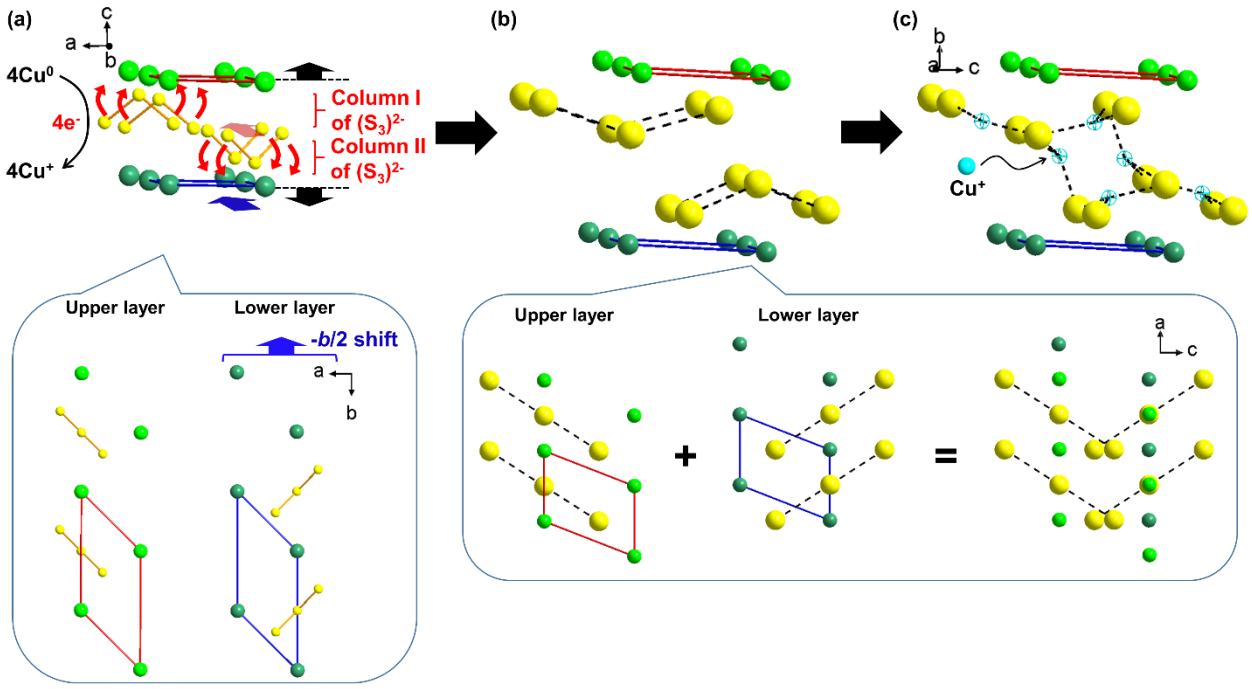


**Figure S13**. Plausible reaction pathway from $BaS_3$ to $BaCu_4S_3$. (a) Structure of $BaS_3$. Upper and lower $Ba^{2+}$ layers are colored by lime and green, respectively. A shift along the $[0\bar{1}0]$ direction of the columns II and the bottom $Ba^{2+}$ layers by - ½ *b* vector leads (b) structure of *β*-$BaCu_4S_3$. Concurrently reduction of $(S_3)^{2-}$ trimers results in their conformational change and S-S bond cleavage to give the trimers represented in the broken lines. (c) Structure of *β*-$BaCu_4S_3$ highlighting trigonal planar/tetrahedral sites for $Cu^+$ cations and Cu-S bonds by cyan hollow spheres and broken lines, respectively.

In $BaS_3$ (SG: *P*-42$_1$*m*), $(S_3)^{2-}$ trimers are located in (001) planes. The anionic species can be regarded as discrete entities stacked along the *b* axis. Two columns are then distinguishable, upper one with downward bending (Column I) and the other with upward bending (Column II) of the trimers. The assembly of the two columns gives rise to the double layer of $(S_3)^{2-}$ trimers sandwiched within a base-centered sub-lattice of $Ba^{2+}$. In the case of $BaS_3$ → $BaCu_4S_3$ transformation, a shift along the $[0\bar{1}0]$ direction by - ½ *b* vector should be applied to columns II and the bottom Ba layers connected to them (Fig. S12). At the same time, stepwise or concerted filling of unoccupied antibonding levels of the $(S_3)^{2-}$ trimers may deform their bent configuration to a linear one before their S-S bond cleavage. Such conformational change of bent trimers made of p-block elements is rationalized not only in molecular viewpoint[15] but also by the existence of the linear $(Se_3)^{4-}$ trimer, which possesses two more electrons per unit than $(S_3)^{2-}$ trimers, in the bulk

$Ba_4Cu_8Se_{13}$ material.[16] Thanks to the deformation, $Cu^+$ cations can be accommodated at the tetrahedral and trigonal planar sites defined from four dumbbells next to each other of four distinct $S_3$ trimers belonging to columns I and II, respectively. The resultant *β*-$BaCu_4S_3$ structures can be converted into α-phase through slight local rearrangements. Preservation of the structural building blocks and of the layered structure asserts the topochemical nature of the process.

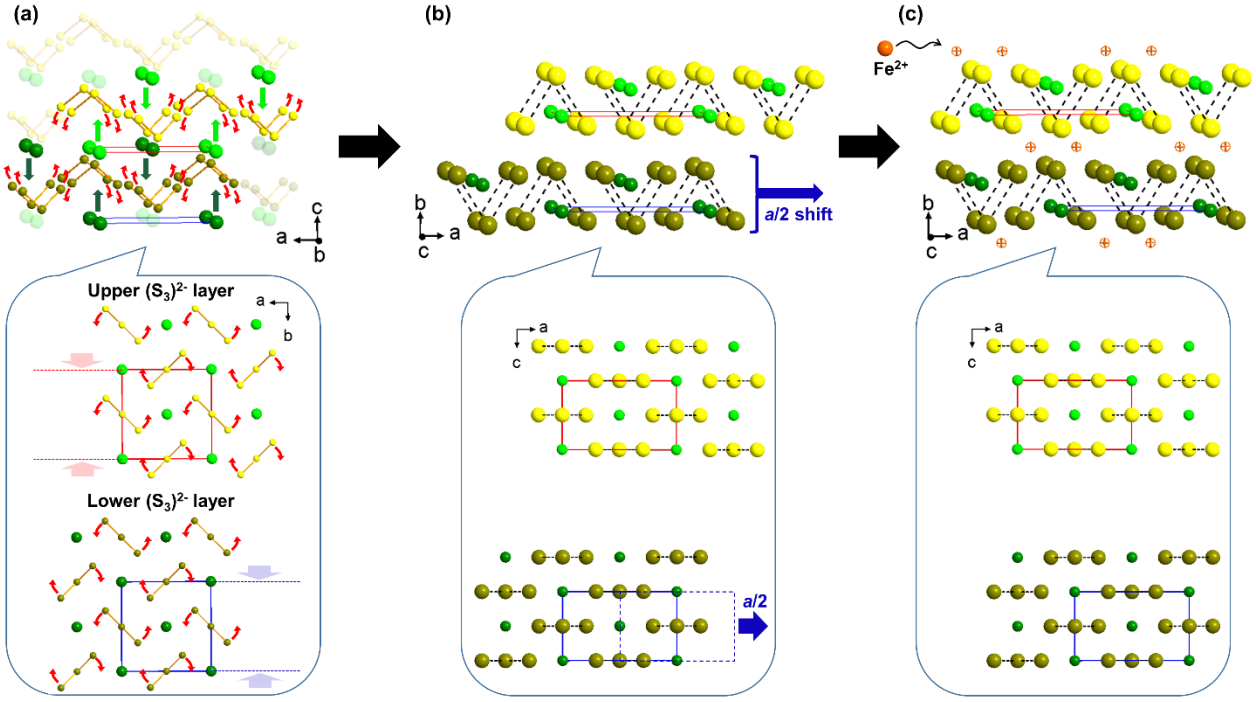


**Figure S14**. Plausible reaction pathway from $BaS_3$ to $BaFe_2S_3$. A red or blue arrow describe movement of each structural unit. (a) Structure of $BaS_3$. $Ba^{2+}$ cations colored lime/deep green are merged into upper/lower $(S_3)^{2-}$ double layers colored yellow/brown, respectively. Concomitant S-S bond breaking leads (b) a hypothetical structure before the transformation to reach the structure of $BaFe_2S_3$ through *a*/2 shift of bottom $^2/_\infty[BaS_3]$ layer. (c) Structure of $BaFe_2S_3$ displaying tetrahedral sites for $Fe^{2+}$ cations by orange hollow spheres.

# References


1. I. Kawada, K. Kato, S. Yamaoka, *Acta Cryst.*, 1975, **B31**, 2905.
2. S. Yamaoka, J. T. Lemley, J. M. Jenks, H. Steinfink, *Inorg. Chem.*, 1975, **14**, 129.
3. V. Petříček, M. Dušek, L. Palatinus, *Z. Für Krist. – Cryst. Mater.*, 2014, **229**, 345.
4. H. E. Swanson, E. Tatge, *Nat. Bur. Stand. Circ.*, 1953, **539**, 1.
5. J. E. Iglesias, K. E. Pachali, H. Steinfink, *J. Solid State Chem.*, 1974, **9**, 6.
6. J. E. Iglesias, K. E. Pachali, H. Steinfink, *Mat. Res. Bull.*, 1972, **7**, 1247.
7. I. E. Grey, H. Steinfink, *J. Am. Chem. Soc.*, 1970, **92**, 5093.
8. T. Petzel, *Z. Anorg. Allg. Chem.*, 1973, **396**, 173.
9. N. Alsén, *GFF*, 1925, **47**, 19.
10. H. Y. Hong, H. Steinfink, *J. Solid State Chem.*, 1972, **5**, 93.
11. E. F. Bertaut, *J. Phys. Radium*, 1954, **15**, 775.
12. R. W. Cheary, A. A. Coelho, *J. Appl. Cryst.*, 1998, **31**, 851.
13. H.-J. Freund, M. W. Robert, *Surf. Sci. Rep.*, 1996, **25**, 225.
14. R. Elliott, R. Compton, R. Levis, S. Matsika, *J. Phys. Chem. A*, 2005, **109**, 11304.
15. M. Morin, A. E. Foti, D. R. Salahub, *Can. J. Chem.*, 1985, **63**, 1982.
16. S. Maier, O. Perez, D. Pelloquin, D. Berthebaud, S. Hébert, F. Gascoin, *Inorg. Chem.*, 2017, **56**, 9209.
17. V. Rajamani, C. T. Prewitt, *Can. Mineral.* 1974, **12**, 248.
18. N. Elliot, *J. Chem. Phys.*, 1960, **33**, 903.
19. H. Seim, H. Fjellvåg, F. Grønvold, S. Stølen, *J. Solid State Chem.*, 1996, **121**, 400.